

Influence of Electron-Donating and Electron-Withdrawing Substituents on the Chemiluminescence Behavior of Coelenterazine Analogs

Ryota Saito,*¹ Takashi Hirano,² Shojiro Maki,² Haruki Niwa,² and Mamoru Ohashi^{2,‡}

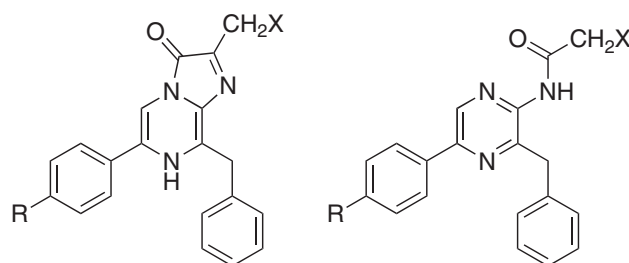
¹Department of Chemistry, Toho University, 2-2-1 Miyama, Funabashi, Chiba 274-8510

²Department of Applied Physics and Chemistry, The University of Electro-Communications, Chofu, Tokyo 182-8585

Received July 5, 2010; E-mail: saito@chem.sci.toho-u.ac.jp

Coelenterazine analogs **3a–3e** possessing various substituents at the *para*-position of the 6-phenyl group (R = CF₃, F, H, OMe, and NMe₂) were synthesized, and the chemiluminescent properties of **3a–3e** in dimethyl sulfoxide (DMSO) were investigated quantitatively. Chemiluminescence maxima observed in the range of 454–478 nm showed a bathochromic shift as the electron-donating ability of R increased. Chemiluminescence quantum yields (Φ_{CL}) were obtained in the range of 0.0006–0.0018. The analog **3a** possessing the electron-withdrawing CF₃ group showed a slight decrease in its Φ_{CL} value. The fluorescence quantum yields (Φ_{F}) of the light emitter, 2-acetamidopyrazine anions **4a⁻–4e⁻**, were observed in the range of 0.005–0.21 and showed substituent dependency in that the increment in the electron-withdrawing ability of R decreases the Φ_{F} value. The efficiency of generation of the singlet-excited **4a⁻–4e⁻** (Φ_{S}) showed a small change in the range of 0.008–0.015. From these quantitative analyses of the quantum efficiencies, we found that an electron-donating substituent R is not required for the efficient generation of a singlet-excited light emitter, but is required for the high Φ_{F} of the emitter.

Coelenterazine (**1**) (Chart 1) is well known as a common luminescent substrate of various luminescent marine organisms.^{1–5} A photoprotein called aequorin, isolated from the jellyfish *Aequorea aequorea*, is one such representative luminescent system that contains **1**. Aequorin is made up of an apoprotein (apoaequorin), **1**, and oxygen. In aequorin, **1** exists as a peroxide which is formed by the reaction of **1** with O₂ at the C2 position.⁶ Upon binding with calcium ions, a conformational change is induced in the protein, after which the peroxide intermediate undergoes the luminescent reaction in the polypeptide environment to yield coelenteramide (**2**) and carbon dioxide. During this bioluminescence reaction, the singlet-excited state of the phenolate anion of **2** is generated and emits blue light ($\lambda_{\text{max}} = 465$ nm). As a chemiluminescence process, **1** also undergoes a reaction with molecular oxygen in an aprotic solvent such as dimethyl sulfoxide (DMSO) without any support of a protein. It has been suggested that the bio- and chemiluminescence reaction of **1** follows the same molecular mechanism as that shown in Scheme 1, in which the thermal decomposition of the 1,2-dioxetanone intermediate (**I**) is an important chemical process in the generation of the electronically excited state of the emitter (**II**). Although the same mechanism is adopted for explaining the bio- and chemiluminescence of **1**, there is a remarkably substantial difference between their luminescence efficiencies. That is, the chemiluminescence efficiency of **1** ($\Phi = 0.002$ in DMSO) is considerably lower than that of aequorin bioluminescence ($\Phi = 0.2$). Quantitative analyses of chemiluminescence quantum yields of coelenterazine-related compounds has revealed that quantum efficiencies in the steps of singlet-excited emitter generation (from **I** to **II**) are very small (0.2–1.5%),^{7,8} while in bioluminescence the singlet-excited emitter is believed to be

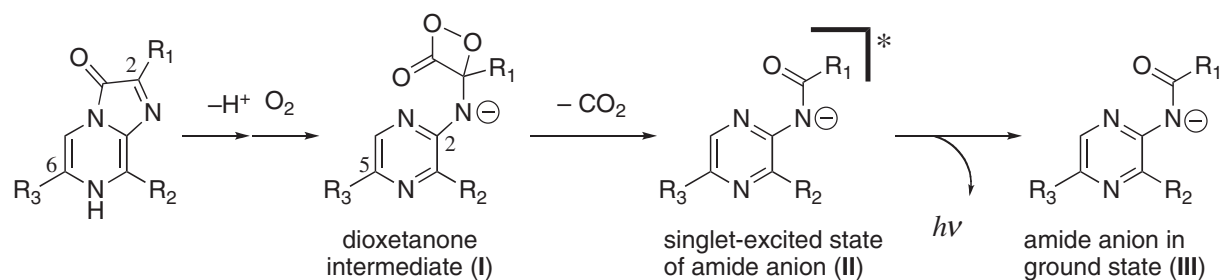


- | | |
|---|---|
| 1: X = C ₆ H ₄ (<i>p</i> -OH), R = OH | 2: X = C ₆ H ₄ (<i>p</i> -OH), R = OH |
| 3a: X = H, R = CF ₃ | 4a: X = H, R = CF ₃ |
| 3b: X = H, R = F | 4b: X = H, R = F |
| 3c: X = H, R = H | 4c: X = H, R = H |
| 3d: X = H, R = OMe | 4d: X = H, R = OMe |
| 3e: X = H, R = NMe ₂ | 4e: X = H, R = NMe ₂ |

Chart 1.

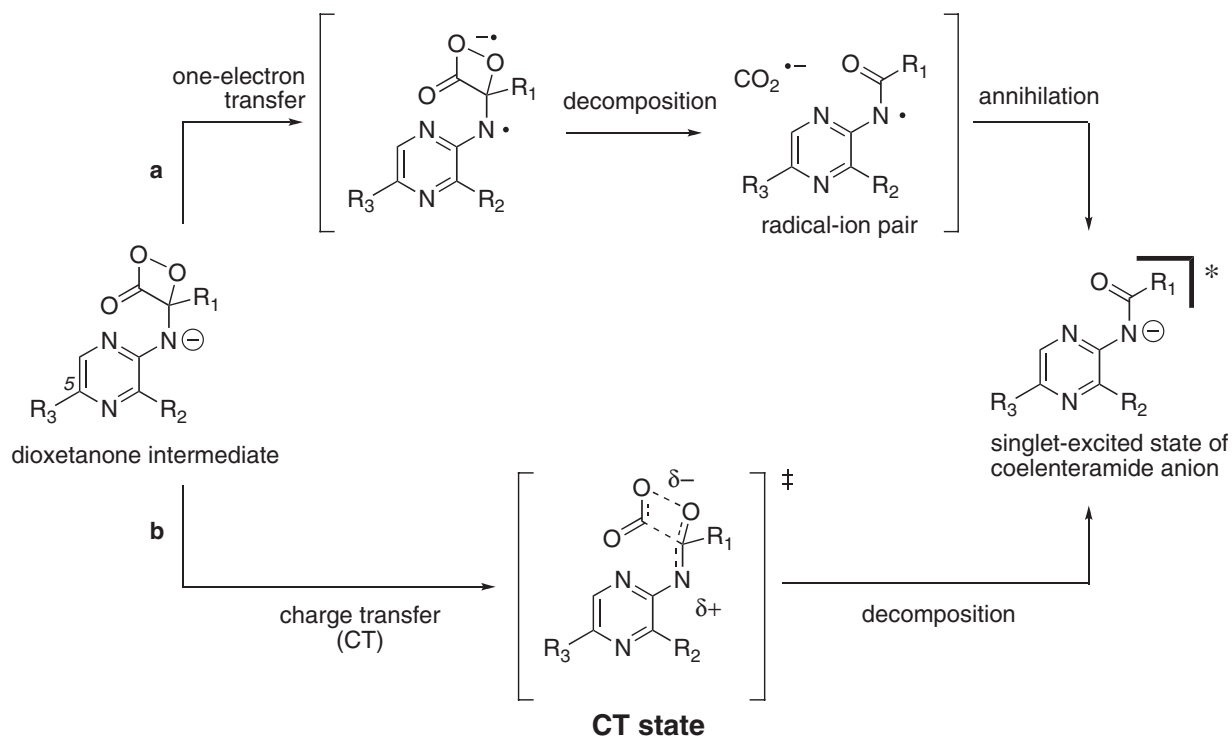
formed quantitatively.⁹ In addition, there have been papers pointing out that the high-quantum-yield bioluminescence involves a high efficiency in the singlet-excited emitter generation.¹⁰ The reason behind the difference in the efficacies of singlet-excited emitter generation has long been the main focus of bio- and chemiluminescence studies and remains a subject of controversy.

To explain the effective generation of singlet-excited molecules in the decomposition of dioxetanone compounds, Schuster proposed a chemically initiated electron exchange luminescence (CIEEL) mechanism that involves complete one-electron transfer, followed by the annihilation of the generated radical ions (Scheme 2a).¹¹ Several reports, however, have demonstrated that CIEEL reactions do not necessarily produce



Scheme 1.

CIEEL mechanism



Scheme 2.

singlet-excited molecules in good yields.¹² As an alternative explanation, it has been suggested that the decomposition of dioxetanone intermediates proceeds via charge-transfer transition states, and not via the completely separated ion pairs, as in the CIEEL mechanism (Scheme 2b).^{12a,13} Although it has not been determined which explanation is correct, both explanations suggest the necessity of a strong electron donor within a molecule for an effective luminescence reaction. Therefore, it is important to determine the bio- and chemiluminescence efficiency of the electron-donating hydroxy group on the 6-phenyl group of **1** by regulating the electronic properties of the reaction intermediates in Scheme 1. In order to experimentally clarify the relevance of an electron-donating substituent at the *para*-position (C4') of the 6-phenyl group for the efficient generation of a singlet-excited emitter in the bioluminescent reactions of **1**, we synthesized coelenterazine analogs **3a–3e** possessing various substituents R (CF₃, F, H, OMe, and NMe₂), whose Hammett substituent constant σ_p was systematically varied, and reported the preliminary results of their chemiluminescence.⁸ Herein, we report the detailed spectroscopic

and chemiluminescent properties of **3a–3e**, and discuss whether or not the electron-donating or electron-withdrawing property of the substituent R essentially effects the efficacy of generating a singlet-excited-state emitter during the oxidative luminescence reaction of **3a–3e**.

Results and Discussion

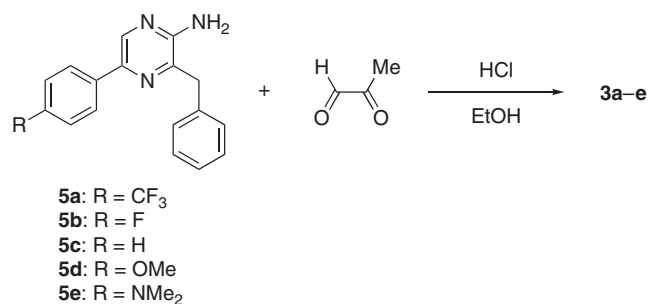
Synthesis and Electronic Absorption Properties of Coelenterazine Analogs. Coelenterazine analogs **3a–3e** were synthesized by the condensation of pyruvaldehyde and the corresponding coelenteramine derivatives **5a–5e**,¹⁴ as shown in Scheme 3. Compounds **6a**, **6c**,¹⁵ and **6d**¹⁶ were also synthesized as references for discussing the electronic absorption properties of **3a–3e** (Scheme 4).

In order to elucidate the electronic effect of the substituent R on the central imidazopyrazinone π -system, electronic absorption spectra of **3a–3e** were measured. The results are listed in Table 1 (see also Figure S1). Each analog showed four transition bands in the region of 200–500 nm. The lowest transition band around 420 nm showed a slight bathochromic

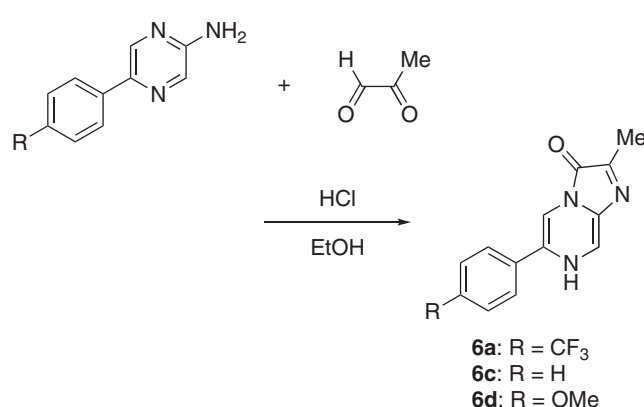
Table 1. Electronic Absorption Data of Coelenterazine Analogs **3a–3e**, **6a**, **6c**, and **6d** in Methanol

Compound (R)	Experimental				Calculated ^{a)}					
	λ_{\max}/nm ($\epsilon/10^3 \text{ dm}^3 \text{ mol}^{-1} \text{ cm}^{-1}$)				λ_{\max}/nm (oscillator strength)					
3a (CF ₃)	420 (sh 0.67)	388 (0.74)	265 (2.19)							
3b (F)	413 (0.65)	352 (0.56)	279 (sh 1.55)	254 (1.97)						
3c (H)	426 (0.84)	358 (0.54)	280 (sh 1.32)	246 (2.12)						
3d (OMe)	427 (0.82)	349 (0.47)	260 (2.23)							
3e (NMe ₂)	432 (0.86)	304 (2.57)	276 (sh 1.40)	223 (sh 1.34)						
6a (CF ₃)	428 (sh 0.64)	377 (0.91)	256 (2.17)		414 (0.27)	361 (0.26)	251 (0.22)	223 (0.50)	204 (0.38)	
6c (H)	424 (0.61)	355 (0.55)	248 (1.80)		422 (0.29)	352 (0.25)	248 (0.26)	223 (0.46)	202 (0.40)	
6d (OMe)	428 (0.73)	351 (0.55)	263 (2.07)		432 (0.30)	346 (0.18)	257 (0.17)	230 (0.33)	205 (0.40)	

a) Calculated as in methanol (dielectric constant $\epsilon = 32.7$) using the INDO/S method. Transitions with oscillator strength less than 0.2 are omitted.

**Scheme 3.**

shift with increasing electron-donating ability of the substituent R. In contrast, the second-lowest-energy transition band around 350 nm is markedly sensitive to the substituent constant of R and showed a hypsochromic shift accompanied by a decrease in the absorption coefficient with increasing electron-donating ability of R. Two other transition bands below 300 nm, which could be assigned to the π - π^* transitions of the 6-phenyl group, tend to separate with increasing electron-donating ability of R. Compounds **6a**, **6c**, and **6d** exhibited the same behavior, suggesting that these absorption bands originate in the π -conjugate system composed of the central imidazopyrazinone skeleton and the 6-phenyl group. Table 1 also lists the computer-simulated electronic transitions of **6a**, **6c**, and **6d** in methanol. In these calculations, the optimized structures of **6a**, **6c**, and **6d** in methanol were first calculated using the AM1-COSMO method.¹⁷ According to these calculations, **6a**, **6c**, and **6d** were found not to take planar structures, and the dihedral angles between the 6-phenyl groups and the central pyrazine were estimated to be 39.0, 40.9, and 41.5°, respectively. With these optimized structures, their electronic excitation spectra were simulated using INDO/S (intermediate neglect of the differential overlap model parameterized for spectroscopy),¹⁸ which is a convenient and widely used method for simulating electronic transition properties of organic dyes.¹⁹ As a result, the second transition band was shifted hypsochromically with an increase in the electron-donating ability of R, a result that coincides with the experimental data. This indicates that these semiempirical calculations provide us with adequate data to understand the substituent effect on the electronic absorption of the imidazopyrazinones. Thus, in order to assign the observed lowest- and second-lowest-energy transition bands for the imidazopyrazinones, the electronic transition of **6c** was further

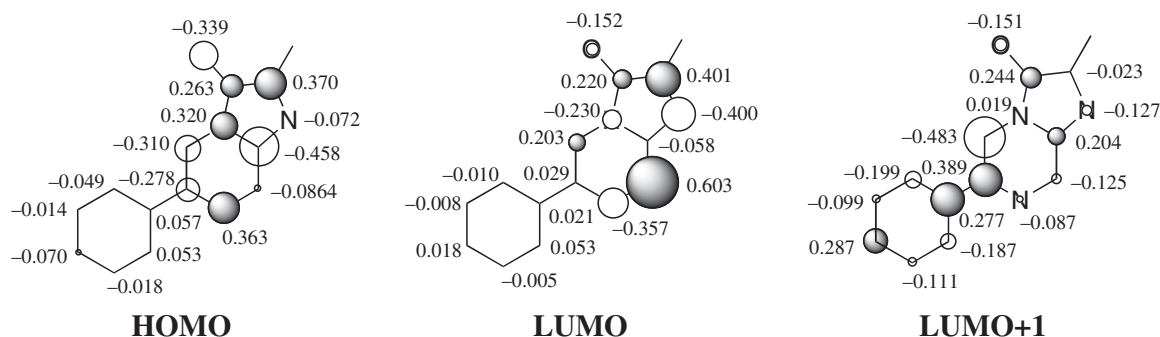
**Scheme 4.**

investigated using the INDO/S method. The results are summarized in Table 2. According to this calculation, the lowest-energy transitions around 420 nm are assignable as the transition between HOMO and LUMO, and the second-lowest-energy transition around 350 nm is assignable as that between HOMO and LUMO+1. Figure 1 shows the HOMO, LUMO, and LUMO+1 of **6c** as obtained by the AM1-COSMO calculation. LUMO+1 has a considerably large electronic distribution on the 6-phenyl group, while HOMO and LUMO have only a negligible electronic distribution on the 6-phenyl group. In particular, LUMO+1 has a large coefficient at C4' of the 6-phenyl group, which indicates that the energy level of LUMO+1 is affected by the substituent R. The LUMO+1 level of **6c** would be elevated by introducing an electron-donating substituent R, thus causing a marked hypsochromic shift of the second-lowest-energy transition. These calculated results well coincide with the observations. From these results, it can be safely said that the second-lowest-energy transitions of **3** and **6** are directly related to the π -conjugations between the central imidazopyrazinone and the 6-phenyl groups. To support this consideration, the effect of the dihedral angle between the imidazopyrazinone skeleton and the 6-phenyl group in **6c** on its absorption maxima was simulated by INDO/S. The results are listed in Table 3. Obviously, the second-lowest-energy transition band was shifted bathochromically with a decrease in the dihedral angle. Similar shifts in the second-lowest-energy absorption bands have been observed with a ring-fused coelenterazine analog, **7** (Chart 2).²⁰ This compound exhibited second-

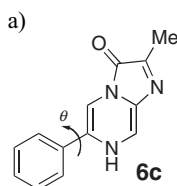
Table 2. Computed Electron Transition Spectra for Singlet State of **6c** in Methanol Calculated by INDO/S Method^{a)}

State	Transition energy		Oscillator strength	Main CSFs MO ^{b)}	CI coefficient ^{c)}
	Energy/eV	Wavelength/nm			
1	2.937	422	0.289	HOMO → LUMO	0.923
2	3.524	352	0.247	HOMO → LUMO+1	0.856
				HOMO → LUMO+3	0.346
3	4.365	284	0.163	HOMO-1 → LUMO	0.820
				HOMO → LUMO+4	0.290
4	4.994	248	0.264	HOMO-1 → LUMO+1	0.744
				HOMO → LUMO+4	0.535

a) Transitions with oscillator strength less than 0.1 are omitted. b) Main configuration state function's molecular orbital; electronic configurations that dominate the corresponding transition energy, as described in terms of their molecular orbitals. c) Absolute configuration interaction coefficient for the CSF.

**Figure 1.** Pertinent molecular orbitals for lowest-energy transition (HOMO → LUMO) and second-lowest-energy transition (HOMO → LUMO+1) of imidazopyrazinone derivative **6c**, calculated using AM1 method. The solvent effect was simulated by use of the COSMO keyword.**Table 3.** Electronic Absorption Spectra as a Function of Dihedral Angle (θ) between the Imidazopyrazinone Skeleton and the 6-Phenyl Group of **6c** Simulated by the INDO/S Method

$\theta/\text{deg}^{\text{a)}$	$\lambda_{\text{max}}/\text{nm}$ (oscillator strength)								
0	421 (0.28)	368 (0.30)	288 (0.16)	256 (0.55)	240 (0.14)	219 (0.25)	202 (0.15)		
15	422 (0.28)	365 (0.29)	288 (0.16)	256 (0.37)	254 (0.16)	241 (0.20)	221 (0.24)	203 (0.15)	
30	422 (0.28)	358 (0.26)	286 (0.17)	251 (0.37)	241 (0.18)	222 (0.34)	201 (0.19)		
40	422 (0.29)	352 (0.25)	284 (0.16)	249 (0.27)	241 (0.17)	223 (0.45)	201 (0.39)		
50	422 (0.29)	346 (0.23)	282 (0.16)	246 (0.16)	241 (0.17)	222 (0.56)	203 (0.14)	202 (0.40)	
60	422 (0.30)	340 (0.21)	281 (0.15)	240 (0.18)	220 (0.61)	202 (0.48)			
75	422 (0.31)	332 (0.18)	279 (0.15)	240 (0.22)	215 (0.51)	203 (0.30)			
90	422 (0.31)	329 (0.18)	278 (-0.16)	239 (0.20)	210 (0.30)				



lowest-energy absorption bands with maxima at longer wavelengths than that of **1**, which indicates that this absorption band is strongly affected by the degree of π -conjugation between the central imidazopyrazinone ring and the 6-phenyl group.

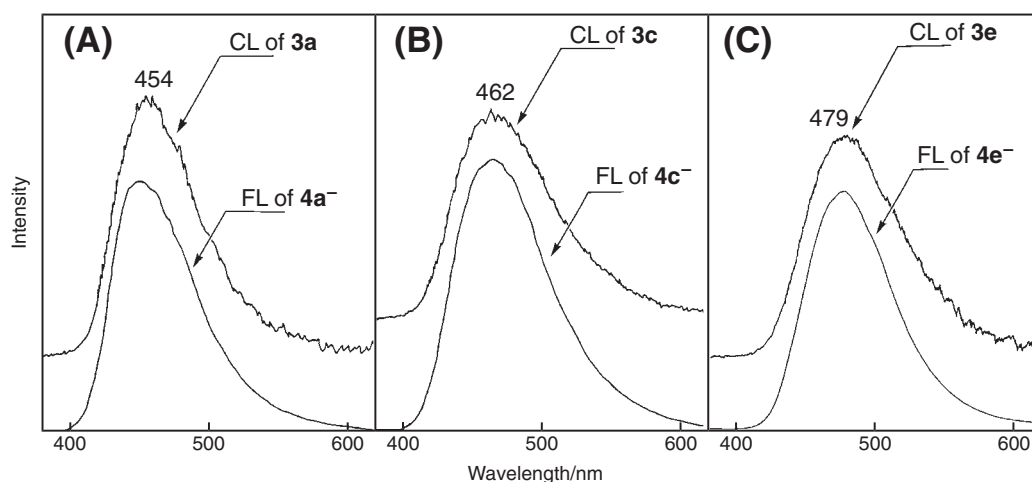
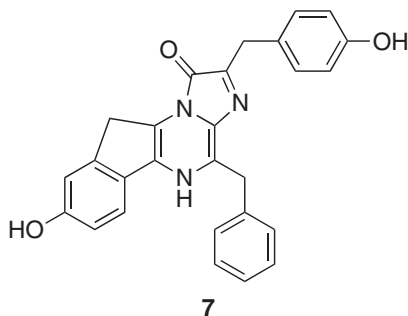
Chemiluminescent Property of 3a–3e in DMSO. Chemiluminescence Emission Maxima: The chemiluminescence of **3a–3e** in DMSO was observed at 25 °C under an aerated condition. In this study, as a solvent we used DMSO, which is

frequently used as a solvent for the chemiluminescence of imidazopyrazinones. The observed emission maxima (CL_{max}) and quantum yields (Φ_{CL}) are summarized in Table 4, accompanied by the fluorescence emission maxima (FL_{max}) of amide anions and neutral forms of the corresponding coelenteramide analogs **4a–4e**.¹⁴ Figure 2 shows representative chemiluminescence spectra of the analogs **3a**, **3c**, and **3e** as well the fluorescence spectra of the amide anions of **4a**, **4c**, and

Table 4. Chemiluminescence Properties of Coelenterazine Analogs **3a–3e** in DMSO and Fluorescence Properties of Coelenteramide Analogs **4a–4e** in DMSO and DMSO Containing 1 M NaOH (0.5% v/v) under Aerated Condition at 25 °C

R	CL _{max} ^{a)} /nm	FL _{max} ^{b)} /nm		Quantum yield			
		In DMSO + NaOH _{aq}	In DMSO	$\Phi_{CL}^{d)}$	$\Phi_R^{e)}$	$\Phi_F^{f)}$	$\Phi_S^{g)}$
CF ₃	454	450	388 ^{c)}	0.0006	0.78	0.05	0.015
F	467	466	376 ^{c)}	0.0015	1.00	0.12	0.012
H	462	462	375 ^{c)}	0.0015	0.93	0.18	0.008
OMe	473	466	396 ^{c)}	0.0018	0.95	0.21	0.009
NMe ₂	479	476	505 ^{c)}	0.0015	0.96	0.19	0.008

a) Chemiluminescence maxima of coelenterazine analogs **3a–3e**. b) Fluorescence maxima of coelenteramide analogs **4a–4e**. c) Values taken from Ref. 14. d) Chemiluminescence quantum yield of coelenterazine analogs **3a–3e** determined on the basis of luminol. e) Chemical yield of the chemiluminescence emitter as determined by HPLC analyses. f) Fluorescence quantum yield of coelenteramide analogs **4a–4e** in DMSO containing 1 M NaOH (0.5% v/v). g) Quantum efficiency of chemical generation of the singlet-excited state of **4a–4e** anion.

**Figure 2.** Selected chemiluminescence spectra (CL) of coelenterazine analogs **3a**, **3c**, and **3e** in DMSO and fluorescence spectra (FL) of coelenteramide analogs **4a**, **4c**, and **4e** in DMSO containing 1 M aqueous NaOH (0.5% v/v): (A) **3a** and **4a**, (B) **3c** and **4c**, and (C) **3e** and **4e**.**Chart 2.**

4e. The result that the CL_{max} values of **3a–3e** matched well with the FL_{max} values of the amide anions of **4a–4e** (Table 4) indicates that the light emitters involved in the chemiluminescent reactions are amide anions **III**, as shown in Scheme 1. The CL_{max} values showed a small but apparent dependency on a change in the substituent R. The CL_{max} value shifted to a longer wavelength region with an increment of the electron-donating

ability of R. In order to evaluate the substituent effect of R on the CL_{max} value more quantitatively, the energies (E_{CL} in kcal mol⁻¹) of the chemiluminescence maxima are plotted against the Hammett substituent constants σ_p of R, as shown in Figure 3. Interestingly, a good correlation between the σ_p and the E_{CL} values is obtained.

To rationalize the observed substituent effect on CL_{max}, the molecular dipoles and the MOs of anionic 2-formamido-5-phenylpyrazines **8** having substituent R (=CF₃, H, and OMe), simple model compounds of the amide anion **4a**⁻, **4c**⁻, and **4d**⁻, were calculated (Figure 4). In these calculations, the geometries of the anionic **8** in the lowest singlet-excited (S₁) states in DMSO were first optimized using the AM1-COSMO method, and then the energy levels of the S₁ state and the corresponding ground states that have the same geometry as the S₁ (S₀^{FC}) state were estimated. Table 5 displays the calculated S₁ and S₀^{FC} levels for the anionic **8** having substituent R (=CF₃, H, and OMe), the differential energies (ΔE in eV) for their S₁ → S₀^{FC} transitions, and the molecular dipole moments for the optimized geometries. The computed ΔE value increased

Table 5. Calculated Molecular Dipole Moments, Energy Levels of the Lowest-Singlet-Excited States (S_1) and the Ground States with Unrelaxed Franck–Condon Geometries (S_0^{FC}), and the Differential Energies (ΔE) for the $S_1 \rightarrow S_0^{\text{FC}}$ Transitions for the Model Compound **8**

Structure of 8	Substituent (R)	Dipole moment/D ^{a)}	Energy level/eV ^{a)}		$\Delta E/\text{eV}^{\text{a)}$
			S_0^{FC}	S_1	
	CF ₃	6.522	-5.971	-3.228	2.880
	H	12.635	-5.788	-3.140	2.711
	OMe	16.841	-5.722	-3.119	2.692

a) Calculated as in DMSO (dielectric constant $\epsilon = 45.0$) by the AM1-COSMO method.

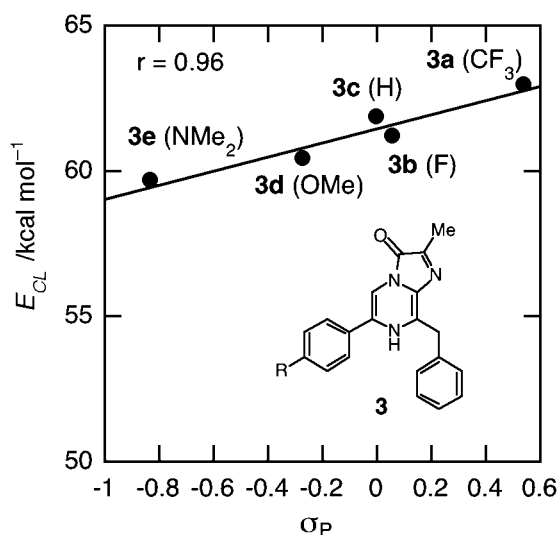


Figure 3. Chemiluminescence energy E_{CL} (in kcal mol^{-1}) of coelenterazine analogs **3a–3e** plotted against Hammett substituent constant σ_{p} .

with the electron-withdrawing trifluoromethyl group and decreased with the electron-donating methoxy group. These results correspond well to the experimentally observed substituent effect. The calculated molecular dipole moment increased sequentially with an increase in the electron-donating ability of the substituent R. The S_1 energies were estimated in the range of -3.228 to -3.119 eV ($\Delta = 0.109$ eV), and the S_0^{FC} energies in the range of -5.971 to -5.722 eV ($\Delta = 0.249$ eV). Both the S_0^{FC} and S_1 energies decreased with an increase in the electron-withdrawing ability of R, which indicates that the introduction of an electron-withdrawing substituent R stabilizes both HOMO and LUMO levels. The larger energy variation in S_0^{FC} ($\Delta = 0.249$ eV) than in S_1 ($\Delta = 0.109$ eV) indicates that the S_0^{FC} states are more susceptible to the electronic effect of substituent R than the S_1 states, and the larger stabilization with trifluoromethyl group enlarges the energy gap between S_0^{FC} and S_1 resulting in hypsochromic shift in the emission wavelength.

These computational results strongly indicate that the observed substituent-dependent CL_{max} can be ascribed not to the molecular dipole change of the amide anions but to large variation in the HOMO levels of the emitters depending on the electronic properties of the substituents.

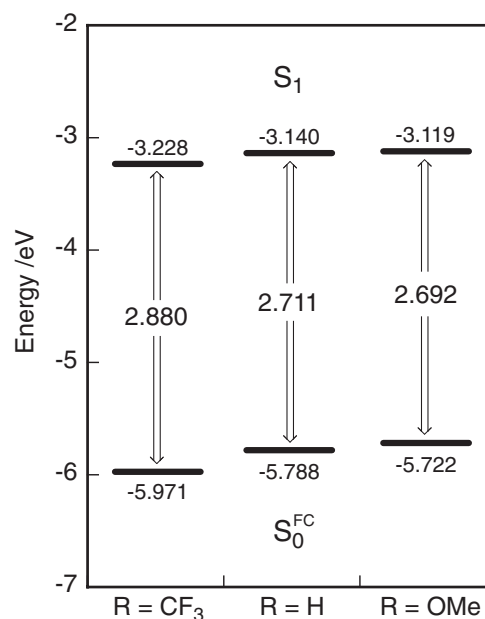


Figure 4. Energy levels of S_0^{FC} and S_1 for **8** ($R = \text{CF}_3$, H, and OMe) calculated as in DMSO ($\epsilon = 45.0$) by the AM1-COSMO method. The $S_0^{\text{FC}}-S_1$ energy gaps are shown with arrows.

Chemiluminescence Efficiency: The chemiluminescence quantum yields (Φ_{CL}) of **3a–3e**, obtained by the measurement of the total number of photons emitted during the course of the chemiluminescence reactions at 25°C under air, are listed in Table 4. The Φ_{CL} values obviously increased with the electron-donating ability of R. The Φ_{CL} value is defined as the product of three yields: the chemical yield of the chemiluminescence emitter (Φ_{R}), the quantum yield of the formation of a singlet-excited light emitter from a high-energy intermediate (Φ_{S}), and the fluorescence quantum yield of a light emitter (Φ_{F}).⁹

$$\Phi_{\text{CL}} = \Phi_{\text{R}} \times \Phi_{\text{S}} \times \Phi_{\text{F}} \quad (1)$$

To clarify the effect of the substituent R on these efficiencies (Φ_{R} , Φ_{S} , and Φ_{F}), we estimated these values for the chemiluminescence reactions of **3a–3e**. The Φ_{R} values were determined as the yields of acetamidopyrazine **4a–4e** by HPLC analyses of the spent products obtained after the chemiluminescence reactions of **3a–3e**. The Φ_{F} values were measured as

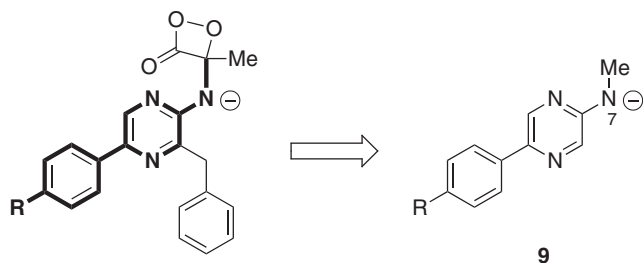


Chart 3.

the fluorescence quantum yields of the amide anions of **4a–4e** in DMSO containing 1 M NaOH aqueous solution (0.5% v/v). By substituting the Φ_{CL} , Φ_R , and Φ_F values in eq 1, the Φ_S values were calculated. These Φ_R , Φ_S , and Φ_F values are compiled in Table 4. Each analog underwent a chemiluminescent reaction to give **4a–4e** in good yield in DMSO under air. The fluorescence quantum yields Φ_F of the **4c–4e** anions were ca 0.2, while the Φ_{FL} of **4a** and **4b** were lower than those of **4c–4e**. Thus, it was proved that an electron-withdrawing R substantially decreases the fluorescence efficiency of the singlet-excited amide anion **III**. Unlike the substituent-sensitive Φ_F , the estimated Φ_S values showed only a small variation in the range of 0.008–0.015 by changing substituents. From these results, it can safely be said that the observed substituent effect on the Φ_{CL} value predominantly reflects the Φ_F change by R.

In order to correlate the obtained Φ_S values with the electronic properties of the central 5-aryl-3-benzylpyrazylaminide anion moiety of the dioxetane intermediate, the net atomic charges, electron densities, and the HOMO coefficients of the nitrogen atom of the aminide anion (designated as N7) of the corresponding model structure **9** (Chart 3) with the substituent R were calculated using the AM1 method. The results are given in Table 6. The absolute HOMO coefficients are estimated in the range of 0.463 to 0.480 eV ($\Delta = 0.017$ eV). The calculated net atomic charges and the electron densities are in the range of -0.450 to -0.470 ($\Delta = 0.020$) and 5.451 to 5.470 ($\Delta = 0.019$), respectively. Thus, in the present imidazopyrazinone chemiluminescence system, the electronic effect of R does not reach the N7, and the small change in the electronic properties of the pyrazylaminide anion moiety can be attributed to the substituent-insensitive Φ_S .

Teranishi and Goto reported the chemiluminescence of 5-(5-aryl-2-pyrazinylamino)-1,2,4-trioxane derivatives **10** (Chart 4), which chemiluminesced in the presence of a base by way of the dioxetane intermediate **11**, and the observed Φ_S values for this system were in the range of 0.0026 to 0.0067.⁷ Based on these results, they claimed that the electron-donating ability of the nitrogen anion in the intermediate **11** was strong enough to accomplish the dioxetane decomposition, which is why no distinct substituent effect was observed. Our present Φ_S values for the chemiluminescence of **3a–3e** demonstrated trends similar to those reported for **10**.

Aequorin bioluminescence shows a high luminescence quantum yield ($\Phi = 0.2$), and therefore the Φ_S value is larger than 0.2. This value is considerably higher than those obtained in the present chemiluminescence system ($\Phi_S = 0.008–0.015$). According to both the CIEEL and the CT mechanisms, strong electron donation from the 6-position in **1** is considered to be

Table 6. Absolute HOMO Coefficients, the Formal Charges and the Atomic Electron Densities on the Nitrogen Atom of the Pyrazylaminide Anion (N7) of the Model Compound **9**

Substituent (R)	Absolute HOMO coefficient ^{a)}	Formal charge ^{a)}	Atomic electron density ^{a)}
CF ₃	0.475	−0.450	5.451
H	0.464	−0.458	5.458
F	0.480	−0.466	5.466
OMe	0.473	−0.469	5.469
NMe ₂	0.463	−0.470	5.470

a) Calculated as in DMSO (dielectric constant $\epsilon = 45.0$) by the AM1-COSMO method.

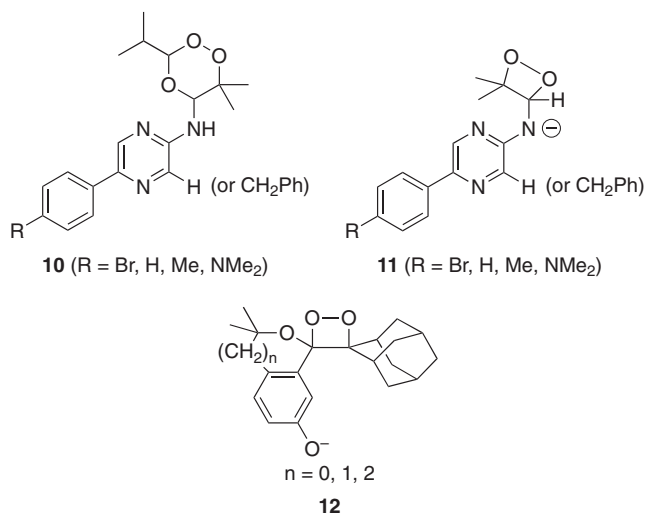


Chart 4.

essential for the high Φ_S value. The importance of the effective electron donation toward the dioxetane ring has already been systematically proven by Schaap et al. for CIEEL-type chemiluminescent 1,2-dioxetanes.²¹ Therefore, there should be another factor that causes such a high Φ_S value in aequorin bioluminescence. One possible explanation for this is that the reactivity of the dioxetane intermediate **II** is regulated not only by the electronic properties of the 5-arylpyrazylaminide anion moiety, but also by the conformation of the dioxetane intermediate. With regard to this, Head and co-workers discovered that the coelenterazine **1** in aequorin is incorporated in the hydrophobic active site of the protein backbone in a peroxidize form, and its orientation is fixed by numerous hydrogen bondings.⁶ In addition, Matsumoto and co-workers reported that the conformation of the electron donor moiety relative to the dioxetane ring in **12** is an important factor for determining the chemiluminescence quantum yield, and they demonstrated that the Φ_S values varied drastically with changes in the dihedral angle between the dioxetane rings and the phenolate anion moiety.²² The importance of the fixed conformation was also pointed out by an ab initio calculation.²³

In light of these facts, we considered the difference between the Φ_S values of aequorin bioluminescence and imidazopyrazinone chemiluminescence systems. We considered that the polypeptide matrix of apoaequorin may effectively regulate the

conformation of the reaction intermediate with the hydrogen-bonding network in such a way that the interaction between the pyrazylamino moiety and the dioxetanone ring is appropriate for a high Φ_S value. However, under chemiluminescence conditions, the most probable conformation of the pyrazylaminide anion relative to the dioxetanone ring could be inappropriate for a high Φ_S value, perhaps owing to the electrostatic repulsion between the anion on the nitrogen and the dioxetanone ring, which is responsible for the observed small Φ_S values and the negligible substituent effect.

Conclusion

We carried out a systematic study of the substituent effect on the chemiluminescent properties of coelenterazine analogs **3a–3e** in DMSO. A quantitative investigation of Φ_{CL} revealed that the Φ_{CL} change was predominantly caused by the variation of the fluorescence efficiency (Φ_F) of the corresponding light emitter, **4a–4e** anion. The Φ_F value showed strong substituent dependency and decreased with the electron-withdrawing ability of R. The generation efficiency of the singlet-excited **4a–4e** anions, on the other hand, was independent of the substituent, and this efficiency was considerably lower than the bioluminescence efficiency of coelenterazine (**1**). These results led us to conclude that it is difficult to develop an efficient imidazopyrazinone-chemiluminescence system that is comparable to aequorin bioluminescence, exploiting only the electronic substituent effect. The chemiluminescence maxima (CL_{max}) were substituent dependent and exhibited a good correlation with the Hammett substituent constant (σ_p) of R. Thus, we found that CL_{max} can be arbitrarily controlled by varying the σ_p value of R.

Experimental

General. All melting points were measured on a MP-21 (Yamato Scientific Co., Ltd., Japan) in open capillary tubes; the values are uncorrected. 1H NMR spectra were recorded on a JNM-GX270 spectrometer (JEOL Ltd., Japan). Chemical shifts (δ) are reported in ppm using tetramethylsilane or an undeuterated solvent as internal standards in the deuterated solvent used. Coupling constants (J) are given in Hz. Chemical shift multiplicities are reported as s = singlet, d = doublet, t = triplet, q = quartet, and m = multiplet. Infrared (IR) spectra were obtained using IR-810 spectrophotometers (JASCO Co., Ltd., Japan). Fast-atom-bombardment (FAB) mass spectra were obtained on a JMS-600-H mass spectrometer (JEOL Ltd., Japan). Xenon was used as a bombardment gas, and all analyses were carried out in positive mode with the ionization energy and the accelerating voltage set at 70 eV and 3 kV, respectively. A mixture of dithiothreitol (DTT) and α -thioglycerol (TG) (1:1 or 1:2) or *m*-nitrobenzyl alcohol (*m*NBA) was used as a liquid matrix. High- and low-resolution electron impact (EI) mass spectra were obtained with a M-80B mass spectrometer (Hitachi Co., Ltd., Japan). The ionization energy and the accelerating voltage were 70 eV and 3 kV, respectively. Column chromatography was carried out on silica gel (63–210- μ m particle size; Kanto Chemical Co.). Semiempirical calculations for ground and singlet-excited states were carried out with the AM1 method^{17a,17b} and the COSMO model^{17c,17d} of MOPAC version 94 incorporated in CAChe software system

(CAChe Scientific Inc.). INDO/S calculations¹⁸ were performed on the ZINDO program incorporated in the CAChe system. For CI calculations, nine occupied molecular orbitals (HOMO–8 to HOMO) and nine unoccupied molecular orbitals (LUMO to LUMO+8) were taken into account. All conventional chemicals used in the present study are commercially available, and were used as received.

Chemiluminescence Spectra. A solution for chemiluminescence measurement was prepared by mixing a stock solution (100 μ L) of 1.0 mM **3a–3e** in methanol and DMSO (2.0 mL) within a quartz cuvette at room temperature. A PMA-10 photonic multichannel analyzer (Hamamatsu Photonics K. K.) was used for recording the chemiluminescence spectra.

Chemiluminescence Quantum Yields. The chemiluminescence quantum yields of **3a–3c** at 25 °C were determined by comparing their luminescence intensities to that of luminol as a standard ($\Phi_{CL} = 0.028$). The luminescence intensities were recorded on a TD-4000 lumiphotometer (Laboscience Co., Tokyo, Japan). The conditions for this experiment were as follows: a 15- μ L methanolic solution of **3a–3c** (4.0 μ M) was placed in the lumiphotometer, and the chemiluminescence reaction was initiated by the injection of 300 μ L of dehydrated DMSO.

UV-vis Absorption and Fluorescence Spectrometry. Spectral grade solvents were used for the measurement of UV-vis absorption and fluorescence spectra. UV-vis spectra were recorded on a Model 320 (Hitachi Co., Ltd., Japan) or a V-550 spectrophotometer (JASCO Co., Ltd., Japan). Fluorescence spectra were measured with a Model F-4010 (Hitachi Co., Ltd., Japan) or a Model F-777 fluorescence spectrophotometer (JASCO Co., Ltd., Japan) and corrected according to the manufacturer's instructions (excitation bandpass: 5 nm; emission band pass: 5 nm; response: 2.0 s; scan speed: 60 nm min⁻¹). A solution of compound **4a–4e** for fluorescence measurement was prepared by mixing a stock solution (100 μ L) of **4a–4e** in DMSO (2.0 mM) and a solvent (2.0 mL) within a 1-cm² quartz cuvette at 25 °C. The reproducibility of each measurement was definitively verified.

Fluorescence Quantum Yields. The fluorescence quantum yields at 25 °C were measured relative to quinine bisulfate in 0.1 M sulfuric acid¹⁴ and calculated on the basis of the following equation:

$$\Phi_f^{sam} = \Phi_f^{ref} \frac{n_{ref}^2}{n_{sam}^2} \frac{OD_{ref}}{OD_{sam}} \frac{\int I_f^{sam}(\lambda_f^{sam}) d\lambda_f^{sam}}{\int I_f^{ref}(\lambda_f^{ref}) d\lambda_f^{ref}}$$

where n_{ref} and n_{sam} are the refractive indices of the solvents, OD_{ref} and OD_{sam} (≤ 0.02) are the optical densities, Φ_f^{ref} ($= 0.52$) and Φ_f^{sam} are the quantum yields, and the integrals denote the (computed) area of the corrected fluorescence spectra, each parameter for the standard (ref) and sample (sam) solutions, respectively. The reproducibility of each measurement was definitively verified.

Determination of Φ_R Values. The Φ_R values were determined by comparing the HPLC chromatogram of the luminescence-spent product with that of the corresponding synthesized acetamidopyrazine **4a–4e**. The HPLC analyses were performed on an Inertsil ODS column (4.6 \times 250 mm; GL Sciences, Inc., Japan) with an acetonitrile/water solvent system as a mobile phase.

8-Benzyl-2-methyl-6-(4-trifluoromethylphenyl)imidazo[1,2-*a*]pyrazin-3(7*H*)-one (3a). To a degassed ethanol solution (4.5 mL) of **5a** (100 mg, 0.30 mmol) was added pyruvaldehyde (40 wt % solution in water, 106 mg, 0.58 mmol) and conc. HCl (50 μ L). The mixture was heated at 80 °C in a sealed vessel under argon atmosphere for 2.5 h. After cooling to room temperature, the solvent was removed under reduced pressure. The resulting yellow residue was purified by column chromatography on silica gel with 10% methanol in dichloromethane as a mobile phase to yield **3a** as yellow solids: yield, 95 mg (83%); mp 134 °C (decomp); ¹H NMR (270 MHz, CD₃OD): δ 2.46 (s, 3H), 4.42 (s, 2H), 7.21–7.43 (m, 5H), 7.78 (d, *J* = 8.4 Hz, 2H), 7.92 (br m, 3H); IR (ν_{\max} (KBr)/cm⁻¹): 3358 (br, ν NH), 3066, 2914 (ν CH), 1638 (ν C=O), 1614, 1552, 1513, 1491 (ν C=C; ring stretching), 1319 (ν CF). HRMS (positive-EI) Calcd for C₂₁H₁₆F₃N₃O: 383.1245. Found: 383.1246.

8-Benzyl-6-(4-fluorophenyl)-2-methylimidazo[1,2-*a*]pyrazin-3(7*H*)-one (3b). This was prepared from **5b** in a procedure analogous to that used to obtain **3a**. The product **3b** was obtained as yellow solids (86%): mp 175 °C (decomp); ¹H NMR (270 MHz, CD₃OD): δ 2.47 (s, 3H), 4.40 (s, 2H), 7.20–7.41 (m, 7H), 7.72 (br m, 3H); IR (ν_{\max} (KBr)/cm⁻¹): 3382 (br, ν NH), 3062, 2914 (ν CH), 1670 (ν C=O), 1594, 1557, 1509 (ν C=C; ring stretching), 1180 (ν CF). HRMS (positive-EI) Calcd for C₂₀H₁₆FN₃O: 333.1277. Found: 333.1278.

8-Benzyl-2-methyl-6-phenylimidazo[1,2-*a*]pyrazin-3(7*H*)-one (3c). This was prepared from **5c** in a procedure analogous to that used to obtain **3a**. The product **3c** was obtained as yellow solids (83%): mp 115 °C (decomp); ¹H NMR (270 MHz, CD₃OD): δ 2.48 (s, 3H), 4.41 (s, 2H), 7.24–7.62 (m, 11H); IR (ν_{\max} (KBr)/cm⁻¹): 3418 (br, ν NH), 3044, 2914 (ν CH), 1671 (ν C=O), 1631, 1556, 1493 (ν C=C; ring stretching), 1180 (ν CF), 872, 694 (ν CH). HRMS (positive-EI) Calcd for C₂₀H₁₇N₃O: 315.1372. Found: 315.1369.

8-Benzyl-6-(4-methoxyphenyl)-2-methylimidazo[1,2-*a*]pyrazin-3(7*H*)-one (3d). This was prepared from **5d** in a procedure analogous to that used to obtain **3a**. The product **3d** was obtained as yellow solids (67%): mp 130 °C (decomp); ¹H NMR (270 MHz, CD₃OD): δ 2.47 (s, 3H), 3.85 (s, 3H), 4.40 (s, 2H), 7.04 (d, *J* = 8.8 Hz, 2H), 7.23–7.41 (m, 5H), 7.56–7.59 (m, 3H); IR (ν_{\max} (KBr)/cm⁻¹): 3426 (br, ν NH), 3164, 3052 (ν CH), 1664 (ν C=O), 1628, 1604, 1538, 1509 (ν C=C; ring stretching), 1024 (ν ArOC). HRMS (positive-EI) Calcd for C₂₁H₁₉N₃O₂: 345.1477. Found: 345.1473.

8-Benzyl-6-(4-dimethylaminophenyl)-2-methylimidazo[1,2-*a*]pyrazin-3(7*H*)-one (3e). This was prepared from **5e** in a procedure analogous to that used to obtain **3a**. The product **3e** was obtained as orange solids (50%): mp 118 °C (decomp); ¹H NMR (270 MHz, CD₃OD): δ 2.46 (s, 3H), 3.00 (s, 6H), 4.40 (s, 2H), 6.80 (d, *J* = 8.7 Hz, 2H), 7.24–7.46 (m, 8H); IR (ν_{\max} (KBr)/cm⁻¹): 3423 (br, ν NH), 3060, 2968 (ν CH), 1624 (ν C=O), 1610, 1569, 1520, 1494 (ν C=C; ring stretching). HRMS (positive-EI) Calcd for C₂₂H₂₂N₄O: 358.1794. Found: 358.1794.

2-Methyl-6-(4-trifluoromethylphenyl)imidazo[1,2-*a*]pyrazin-3(7*H*)-one (6a). This was prepared from 2-amino-5-(4-trifluoromethylphenyl)pyrazine²⁴ in a procedure analogous to that used to obtain **3a**. The product **6a** was obtained as yellow

solids (83%): mp 134 °C (decomp); ¹H NMR (270 MHz, CD₃OD): δ 2.45 (s, 3H), 7.83 (d, *J* = 8.4 Hz, 2H), 7.90–8.05 (m, 4H); IR (ν_{\max} (KBr)/cm⁻¹): 3420 (br, ν NH), 3080, 2930 (ν CH), 1675 (ν C=O), 1620 (ν C=C), 1326 (ν CF). HRMS (positive-EI) Calcd for C₁₄H₁₀F₃N₃O: 293.0776. Found: 293.0763.

The authors gratefully acknowledge support for this research by a Grant-in-Aid for Scientific Research from the Ministry of Education, Culture, Sports, Science and Technology of Japan (MEXT). Financial support to R.S. by “High-Tech Research Center” Project for Private Universities: matching fund subsidy from the MEXT and by the Faculty of Science Special Grant for Promoting Scientific Research at Toho University are also gratefully appreciated.

Supporting Information

Absorption spectra of **3a–3e** in methanol (Figure S1) are available. This material is available free of charge on the web at <http://www.csj.jp/journals/bcsj/>.

References

- # Currently a professor emeritus.
- O. Shimomura, S. Inoue, F. H. Johnson, Y. Haneda, *Comp. Biochem. Physiol., Part B: Biochem. Mol. Biol.* **1980**, *65*, 435.
- F. McCapra, R. Hart, *Nature* **1980**, *286*, 660.
- A. K. Campbell, P. J. Herring, *Mar. Biol.* **1990**, *104*, 219.
- O. Shimomura, F. H. Johnson, Y. Saiga, *J. Cell. Comp. Physiol.* **1962**, *59*, 223.
- a) J. C. Matthews, K. Hori, M. J. Cormier, *Biochemistry* **1977**, *16*, 5217. b) R. C. Hart, J. C. Matthews, K. Hori, M. J. Cormier, *Biochemistry* **1979**, *18*, 2204.
- J. F. Head, S. Inouye, K. Teranishi, O. Shimomura, *Nature* **2000**, *405*, 372.
- K. Teranishi, T. Goto, *Bull. Chem. Soc. Jpn.* **1989**, *62*, 2009.
- R. Saito, T. Hirano, H. Niwa, M. Ohashi, *Chem. Lett.* **1998**, 95.
- F. McCapra, *Proc. R. Soc. London, Ser. B* **1982**, *215*, 247.
- a) Y. Takahashi, H. Kondo, S. Maki, H. Niwa, H. Ikeda, T. Hirano, *Tetrahedron Lett.* **2006**, *47*, 6057. b) T. Hirano, Y. Takahashi, H. Kondo, S. Maki, S. Kojima, H. Ikeda, H. Niwa, *Photochem. Photobiol. Sci.* **2008**, *7*, 197.
- a) J.-Y. Koo, G. B. Schuster, *J. Am. Chem. Soc.* **1977**, *99*, 6107. b) F. McCapra, *J. Chem. Soc., Chem. Commun.* **1977**, 946. c) S. P. Schmidt, G. B. Schuster, *J. Am. Chem. Soc.* **1978**, *100*, 1966. d) J.-Y. Koo, G. B. Schuster, *J. Am. Chem. Soc.* **1978**, *100*, 4496. e) G. B. Schuster, B. Dixon, J.-Y. Koo, S. P. Schmidt, J. P. Smith, *Photochem. Photobiol.* **1979**, *30*, 17.
- a) L. H. Catalani, T. Wilson, *J. Am. Chem. Soc.* **1989**, *111*, 2633. b) T. W. Kaaret, T. C. Bruice, *Photochem. Photobiol.* **1990**, *51*, 629.
- a) H. Isobe, Y. Takano, M. Okumura, S. Kuramitsu, K. Yamaguchi, *J. Am. Chem. Soc.* **2005**, *127*, 8667. b) H. Isobe, S. Yamanaka, S. Kuramitsu, K. Yamaguchi, *J. Am. Chem. Soc.* **2008**, *130*, 132.
- R. Saito, T. Hirano, H. Niwa, M. Ohashi, *J. Chem. Soc., Perkin Trans. 2* **1997**, 1711.
- T. Goto, *Pure Appl. Chem.* **1968**, *17*, 421.
- Y. Toya, T. Kayano, K. Sato, T. Goto, *Bull. Chem. Soc. Jpn.*

1992, 65, 2475.

17 a) M. J. S. Dewar, E. G. Zoebisch, E. F. Healy, J. J. P. Stewart, *J. Am. Chem. Soc.* **1985**, 107, 3902. b) M. J. S. Dewar, E. G. Zoebisch, *THEOCHEM* **1988**, 180, 1. c) A. Klamt, G. Schüürmann, *J. Chem. Soc., Perkin Trans. 2* **1993**, 799. d) K. Mori, S. Maki, H. Niwa, H. Ikeda, T. Hirano, *Tetrahedron* **2006**, 62, 6272.

18 a) J. Ridley, M. Zerner, *Theor. Chim. Acta* **1973**, 32, 111. b) A. D. Bacon, M. C. Zerner, *Theor. Chim. Acta* **1979**, 53, 21. c) M. C. Zerner, G. H. Loew, R. F. Kirchner, U. T. Mueller-Westerhoff, *J. Am. Chem. Soc.* **1980**, 102, 589.

19 a) D. Young, *Computational Chemistry: A Practical Guide for Applying Techniques to Real World Problems*, John Wiley & Sons, New York, **2001**. b) M. Adachi, Y. Murata, S. Nakamura, *J. Am. Chem. Soc.* **1993**, 115, 4331. c) M. Belletête, M. Leclerc, G. Durocher, *J. Phys. Chem.* **1994**, 98, 9450. d) C. D. Mitchell, T. L.

Netzel, *J. Phys. Chem. B* **2000**, 104, 125. e) A. A. Voityuk, *Chem. Phys. Lett.* **2006**, 427, 177.

20 K. Teranishi, T. Goto, *Bull. Chem. Soc. Jpn.* **1990**, 63, 3132.

21 a) K. A. Zaklika, A. L. Thayer, A. P. Schaap, *J. Am. Chem. Soc.* **1978**, 100, 4916. b) K. A. Zaklika, T. Kissel, A. L. Thayer, P. A. Burns, A. P. Schaap, *Photochem. Photobiol.* **1979**, 30, 35.

22 M. Matsumoto, N. Watanabe, T. Shiono, H. Suganuma, J. Matsubara, *Tetrahedron Lett.* **1997**, 38, 5825.

23 Y. Takano, T. Tsunesada, H. Isobe, Y. Yoshioka, K. Yamaguchi, I. Saito, *Bull. Chem. Soc. Jpn.* **1999**, 72, 213.

24 R. Saito, E. Iwasa, A. Katoh, in *Bioluminescence & Chemiluminescence: Progress and Perspectives (Proceedings of the 13th International Symposium)*, ed. by A. Tsuji, M. Matsumono, M. Maeda, L. J. Kricka, P. E. Stanley, World Scientific, Singapore, **2005**, pp. 125–128.